Chapter 4

Synergistic growth inhibition based on small-molecule p53 activation as treatment for intraocular melanoma

J. de Lange[1], L.V. Ly[2], K. Lodder[1], M. Verlaan - de Vries[1], A.F.A.S. Teunisse[1], M.J. Jager[1], A.G. Jochemsen[1]

[1] Department of Molecular Cell Biology, Leiden University Medical Center, 2300 RC Leiden, The Netherlands
[2] Department of Ophtalmology, Leiden University Medical Center, 2300 RC Leiden, The Netherlands

Oncogene 2012 Mar 1;31(9):1105-16

Abstract

The prognosis for patients with uveal melanoma is poor. Because of the limited efficacy of current treatments, new therapeutic strategies need to be developed. Because p53 mutations are uncommon in uveal melanoma, reactivation of p53 may be used to achieve tumor regression. We investigated the use of combination therapies for intraocular melanoma, based on the p53 activators Nutlin-3 and reactivation of p53 and induction of tumor cell apoptosis (RITA) and the topoisomerase I inhibitor Topotecan. Nutlin-3 treatment induced p53-dependent growth inhibition in human uveal melanoma cell lines. The sensitivity to Nutlin-3 of the investigated cell lines did not correlate with basal Hdm2 or Hdmx levels. Nutlin-3 synergized with RITA and Topotecan to induce apoptosis in uveal melanoma cell lines and short term cultures. Drug synergy correlated with enhanced induction of p53-Ser46 phosphorylation, which was attenuated by ATM inhibition. Nutlin-3 and Topotecan also significantly delayed tumor growth *in vivo* in a murine B16F10 model for ocular melanoma. Combination treatment appeared to inhibit tumor growth slightly more efficient than either drug alone. Nutlin-3, RITA and Topotecan lead to comparable p53 activation and growth inhibition under normoxia and hypoxia. Treatment with Nutlin-3 or RITA had no effect on HIF-1α induction by hypoxia, whereas the combination of these two drugs did inhibit hypoxia-induced HIF-1α. Also Topotecan, alone or in combination with Nutlin-3, reduced HIF-1α protein levels, suggesting that a certain level of DNA damage response is required for p53-mediated down-regulation of HIF-1α. In conclusion, combination treatments based on small-molecule induced p53 activation may have clinical potential for uveal melanoma.

Introduction

The eye is the second most common site of malignant melanoma, comprising 5.3% of all melanoma cases (Chang *et al.*, 1998). Up to 50% of patients with uveal melanoma may develop metastases. Prognosis is poor when the tumor has metastasized; median survival is about 10 - 18 months (Kivela *et al.*, 2006; Augsburger *et al.*, 2009). Functional inactivation of the p53 tumor suppressor pathway is believed to be involved in virtually all human cancers. The *p53* gene is directly mutated in about 50% of human malignancies, whereas tumors retaining wild type p53 contain other genetic aberrations that prevent p53's tumor suppressor function (Wynford-Thomas and Blaydes 1998). It is generally assumed that p53 mutations in uveal melanoma are rare. The presence of wild type, but functionally impaired p53 and intact downstream signaling may provide an attractive therapeutic strategy to target tumor cells by restoring p53 activity. To this end, small-molecule compounds have been developed, such as the Hdm2 antagonist Nutlin-3 (Vassilev *et al.*, 2004). Specifically, Nutlin-3 binds Hdm2 in its p53-binding pocket, thereby inhibiting Hdm2-p53 interaction, which releases, stabilizes and activates p53. Nutlin-3 activates p53 without inducing DNA damage, making it a non-genotoxic agent (Vassilev, 2007). Normal cells are relatively insensitive to Nutlin-3-induced apoptosis. The p53-binding molecule RITA (reactivation of p53 and induction of tumor cell apoptosis) was described to induce p53-dependent apoptosis and to inhibit tumor growth *in vivo* (Issaeva *et al.*, 2004). RITA was proposed to induce conformational changes in p53, leading to reduced p53-Hdm2 binding. Although this mechanism was questioned by a later study (Krajewski *et al.*, 2005), a more recent report supports it (Enge *et al.*, 2009).

Several groups included Nutlin-3 in combination treatments, mostly together with genotoxic drugs, to enhance their effectiveness and allow such drugs to be administered at lower doses (Coll-Mulet *et al.*, 2006; Lam *et al.*, 2010; Kojima *et al.*, 2006; Barbieri *et al.*, 2006). Those studies showed that in certain experimental settings, synergistic induction of apoptosis can be achieved. The use of Nutlin-3 appeared promising in retinoblastoma treatment (Laurie *et al.*, 2006). Notably, subconjunctival delivery of Nutlin-3, especially in combination with Topotecan, strongly inhibited growth of Y79 human retinoblastoma cells injected into the eyes of newborn rats. Topotecan, frequently used as chemotherapeutic agent, is a topoisomerase I inhibitor that induces double-strand DNA breaks, stimulates p53 phosphorylation, but also triggers apoptosis in p53-deficient cells (Tomicic *et al.*, 2010). The results with retinoblastoma suggest that subconjunctival delivery of Nutlin-3 and Topotecan may also be used in uveal melanoma.

We investigated the use of p53-activating drugs as treatment for uveal melanoma. Our data show that Nutlin-3 induces p53-dependent growth inhibition and synergizes with both RITA and Topotecan to induce apoptosis in uveal melanoma cell lines and short-term cultures. Furthermore, Nutlin-3 and Topotecan inhibited *in vivo* growth of B16F10 cells in a murine model for ocular melanoma. We found similar p53 activation by the various treatments under normoxic and hypoxic conditions. Together, our results indicate that p53 activators have promise in treating primary uveal melanoma and its metastases.

Results

Nutlin-3 activates p53 and inhibits cell growth in uveal melanoma cell lines

To examine whether Nutlin-3 can inhibit the growth of uveal melanoma cell lines 92.1 and Mel202 in a p53-dependent manner, we first generated stable shp53 and shCtrl cell lines. We treated the resulting cell lines with Nutlin-3 and analyzed protein (Figure 1a) and mRNA (Figure 1b) levels. In shCtrl cells, treatment with Nutlin-3 resulted in increased p53 protein levels and upregulation of p53 target genes *Hdm2*, *PUMA* and *p21* at both mRNA and protein level, as expected. In shp53 cells, expressing much lower p53 levels, induction of p53 targets was strongly diminished, showing that the effect of Nutlin-3 is p53 dependent. We examined cell growth using a WST-1 proliferation assay. Nutlin-3 significantly inhibited growth of shCtrl cells, whereas shp53 cells were largely unaffected (Figure 1c).

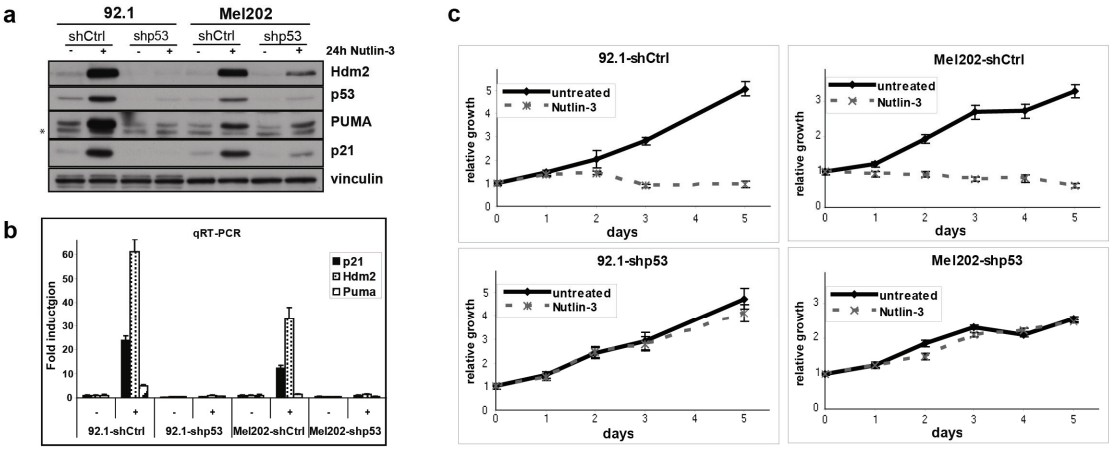

Figure 1 Nutlin-3 activates p53 and inhibits cell growth in uveal melanoma cell lines. The 92.1 and Mel202 cells stably expressing shCtrl or shp53 RNAs were treated with 10 μM Nutlin-3 for 24 h, followed by western blot analysis (**a**) and qRT-PCR (**b**). * Non-specific background staining. (**c**) Cells were counted, seeded for WST-1 proliferation assay and treated with 10 μM Nutlin-3. Cell viability was measured at 0, 24, 48, 72, 96, and 120 h upon Nutlin-3 addition.

In an earlier examination of levels of several proteins in uveal melanoma cell lines, we had observed relatively high levels of Hdmx in 92.1 and Mel202, whereas Mel285 and Mel270 contain high levels of Hdm2 compared with Mel202 and 92.1 cells (Supplementary Figure 1a). Because Hdm2 and Hdmx levels may affect the sensitivity to Nutlin-3 (Patton *et al.*, 2006; Wade *et al.*, 2006; Hu *et al.*, 2006), we tested whether this also applies for uveal

a

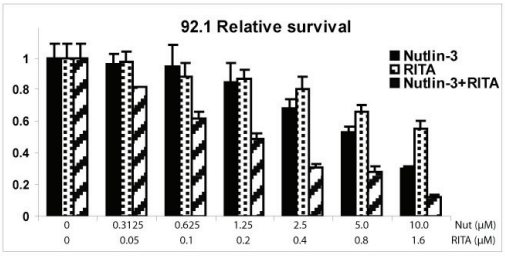

Nutlin-3 Dose (μM)	Effect	RITA Dose (μM)	Effect	Combination N+R Effect	CI
0.3125	0.036	0.05	0.024	0.182	0.356
0.625	0.052	0.1	0.115	0.382	0.276
1.25	0.155	0.2	0.134	0.516	0.338
2.5	0.318	0.4	0.194	0.691	0.348
5	0.470	0.8	0.343	0.718	0.620
10	0.700	1.6	0.445	0.875	0.509
IC50	5.15 μM	IC50	1.74 μM		
m	1.23	m	0.91		
r	0.994	r	0.960		

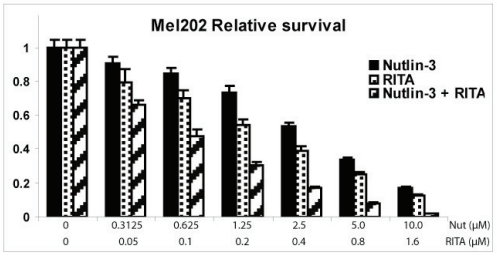

Nutlin-3 Dose (μM)	Effect	RITA Dose (μM)	Effect	Combination N+R Effect	CI
0.3125	0.092	0.05	0.208	0.336	0.653
0.625	0.155	0.1	0.297	0.525	0.599
1.25	0.265	0.2	0.458	0.696	0.583
2.5	0.467	0.4	0.609	0.825	0.567
5	0.664	0.8	0.751	0.919	0.476
10	0.827	1.6	0.876	0.982	0.212
IC50	2.71 μM	IC50	0.23 μM		
m	1.12	m	0.95		
r	0.997	r	0.997		

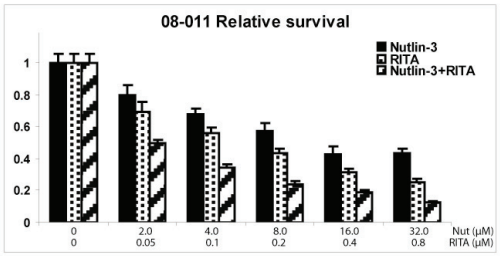

Nutlin-3 Dose (μM)	Effect	RITA Dose (μM)	Effect	Combination N+R Effect	CI
2	0.200	0.05	0.304	0.504	0.467
4	0.319	0.1	0.439	0.657	0.367
8	0.425	0.2	0.569	0.759	0.354
16	0.571	0.4	0.684	0.814	0.441
32	0.569	0.8	0.750	0.872	0.463
IC50	14.49 μM	IC50	0.15 μM		
m	0.63	m	0.7		
r	0.969	r	0.995		

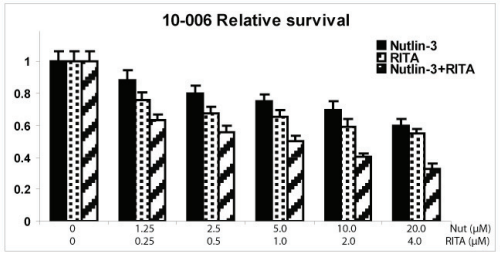

Nutlin-3 Dose (μM)	Effect	RITA Dose (μM)	Effect	Combination N+R Effect	CI
1.25	0.114	0.25	0.239	0.364	0.293
2.5	0.197	0.5	0.323	0.443	0.258
50	0.248	1	0.345	0.500	0.284
10	0.305	2	0.411	0.596	0.226
20	0.404	4	0.450	0.674	0.211
IC50	38.88 μM	IC50	6.46 μM		
m	0.56	m	0.33		
r	0.987	r	0.981		

Figure 2 Synergistic growth inhibition by Nutlin-3 in combination with RITA or Topotecan. The 92.1, Mel202, 08-011 and 10-006 cells were counted and seeded for WST-1 proliferation assay. Cells were treated as indicated with different concentrations, alone or in constant ratio combinations, of Nutlin-3 and RITA (**a**) or Nutlin-3 and Topotecan (**b**). Cell viability was measured after 72 h treatment. The effects of drug treatment as

melanoma. In a WST-1 proliferation assay (Supplementary Figure 1b) we observed comparable Nutlin-3 responses in Mel285 and Mel270 as those found in 92.1 and Mel202. In 92.1, Mel202 and Mel270, but not in Mel285, morphology changes suggested apoptosis induction in a proportion of cells (Supplementary Figure 1c). These findings indicate a lack of correlation between basal Hdm2 or Hdmx levels and sensitivity to Nutlin-3 in the cells examined.

b

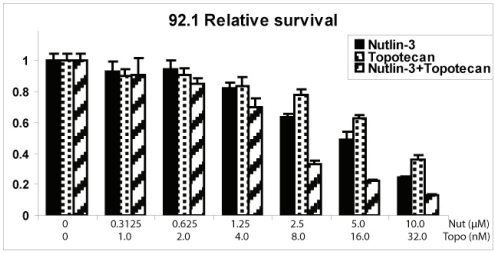

Nutlin-3 Dose (μM)	Effect	Topotecan Dose (nM)	Effect	Combination N+T Effect	CI
0.3125	0.071	1	0.096	0.093	1.164
0.625	0.059	2	0.093	0.152	1.276
1.25	0.176	4	0.161	0.298	1.045
2.5	0.369	8	0.219	0.667	0.444
5	0.513	16	0.370	0.779	0.513
10	0.753	32	0.641	0.872	0.548
IC50	4.38 μM	IC50	25.78 nM		
m	1.15	m	0.81		
r	0.976	r	0.957		

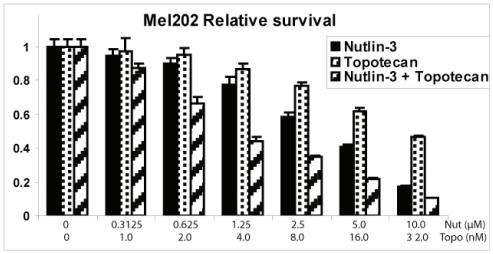

Nutlin-3 Dose (μM)	Effect	Topotecan Dose (nM)	Effect	Combination N+T Effect	CI
0.3125	0.054	1	0.025	0.123	0.670
0.625	0.097	2	0.047	0.333	0.475
1.25	0.221	4	0.130	0.557	0.446
2.5	0.413	8	0.230	0.649	0.652
5	0.596	16	0.382	0.783	0.755
10	0.829	32	0.534	0.896	0.747
IC50	3.28 μM	IC50	25.42 nM		
m	1.28	m	1.12		
r	0.997	r	0.996		

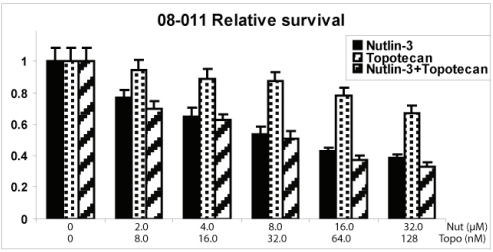

Nutlin-3 Dose (μM)	Effect	Topotecan Dose (nM)	Effect	Combination N+T Effect	CI
2	0.229	8	0.057	0.303	0.708
4	0.348	16	0.108	0.373	0.864
8	0.461	32	0.122	0.490	0.807
16	0.573	64	0.217	0.627	0.667
32	0.617	128	0.327	0.670	0.993
IC50	11.88 μM	IC50	376.27 nM		
m	0.62	m	0.72		
r	0.986	r	0.987		

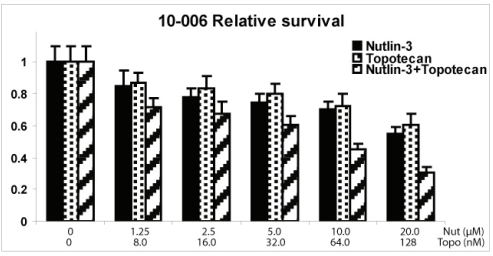

Nutlin-3 Dose (μM)	Effect	Topotecan Dose (nM)	Effect	Combination N+T Effect	CI
1.25	0.149	8	0.129	0.282	0.343
2.5	0.220	16	0.165	0.327	0.454
50	0.256	32	0.200	0.397	0.506
10	0.300	64	0.277	0.550	0.303
20	0.452	128	0.394	0.692	0.186
IC50	37.25 μM	IC50	357.90 nM		
m	0.51	m	0.52		
r	0.976	r	0.987		

fraction of mock-treated control cells were calculated. The dose-response values IC50 (dose required for median effect), *m* (slope signifying the shape of the dose-response curve) and *r* (linear correlation coefficient; *r* = 1 indicates perfect fit) for each single drug were derived using Compusyn software (Chou and Martin, 2007). Based on these values, the CI was derived for each drug combination, reflecting the extent of synergy or antagonism for two drugs. CI<0.9, synergy; 0.9<CI<1.1, additive effect; CI>1.1, antagonism.

Synergistic growth inhibition by Nutlin-3 in combination with RITA or Topotecan

The use of Nutlin-3 alone may not be sufficient to achieve full tumor regression. Combination with other drugs could well enhance the effectiveness of treatment. We analyzed the sensitivity of 92.1 and Mel202 cells to combinations of Nutlin-3 with either RITA or Topotecan. We performed synergy studies using the method of Chou (Chou, 2006). Dose-effect analyses are shown in Figure 2. Nutlin-3 and RITA synergized in both cell lines, with synergy confirmed by calculation of the CI. This is in line with recent findings in multiple myeloma (Saha *et al*., 2010). Nutlin-3 and Topotecan combinations also showed synergistic growth inhibition at most concentrations, except when using low doses in 92.1 cells. We extended our studies to two short-term uveal melanoma cultures, because these should more closely resemble 'real' tumor behavior than fully established cell lines. Short-term cultures 10-006 and 08-011 were also synergistically inhibited by the combination treatments (Figure 2 and Supplementary Figure 2).

To further investigate the cellular responses to the different treatments, we applied flow cytometry (Figure 3a). Nutlin-3 mainly induced G1 arrest, whereas RITA preferentially increased the G2/M fraction. When applied as single treatment, the used doses of Nutlin-3 and RITA only induced a modest sub-G1 increase. This was significantly enhanced in the combination treatment. Topotecan treatment resulted in a G1 reduction and in more cells in S and G2/M phase. A closer examination of the kinetics of this response (Supplementary Figure 3) showed that Topotecan treatment slows down the process of DNA replication. We observed no sustained S-phase arrest, but cells eventually arrested in G2. Combining Topotecan with Nutlin-3 maintained a substantial G1 fraction, and prevented a robust G2 arrest. The increasing S-phase may reflect a 'real' S-arrest or, more likely, dying G2 cells that form a so-called 'sub-G2' fraction. Importantly, sub-G1 fractions were strongly increased in the combination treatment compared with the single treatments. In addition to the enhanced sub-G1 fractions, we found increased Annexin V staining in Nutlin-3 + RITA and Nutlin-3 + Topotecan-treated cells, confirming enhanced induction of apoptosis (Figure 3b).

We analyzed the levels of a number of proteins by western blot (Figure 3c). The levels of various markers of apoptosis, including cleaved PARP, cleaved caspase 3 and p53-Ser46 phosphorylation, were elevated in the combination treated cells, further underscoring that the combination treatments shifted the cellular response from cell cycle arrest to apoptosis. Combination treatments also induced p53-Ser46 phosphorylation in short-term cultures 08-011 and 10-006 (Supplementary Figure 2). Tightly controlled phosphorylation

events are crucial for modulating the p53 response; specifically phosphorylation of serine 46 is believed to result in apoptosis induction (Bulavin *et al.*, 1999; Saito *et al.*, 2002). Therefore, identifying the kinase(s) involved in p53-Ser46 phosphorylation may provide more insight in how apoptosis is triggered. Because RITA has been reported to increase HIPK2 levels, a kinase for p53-Ser46 (D'Orazi *et al.*, 2002; Rinaldo *et al.*, 2009), HIPK2 could be involved. However, in our settings RITA treatment did not lead to HIPK2 induction (Figure 3c). Therefore, the kinase activity of HIPK2 is probably not required for the observed effects.

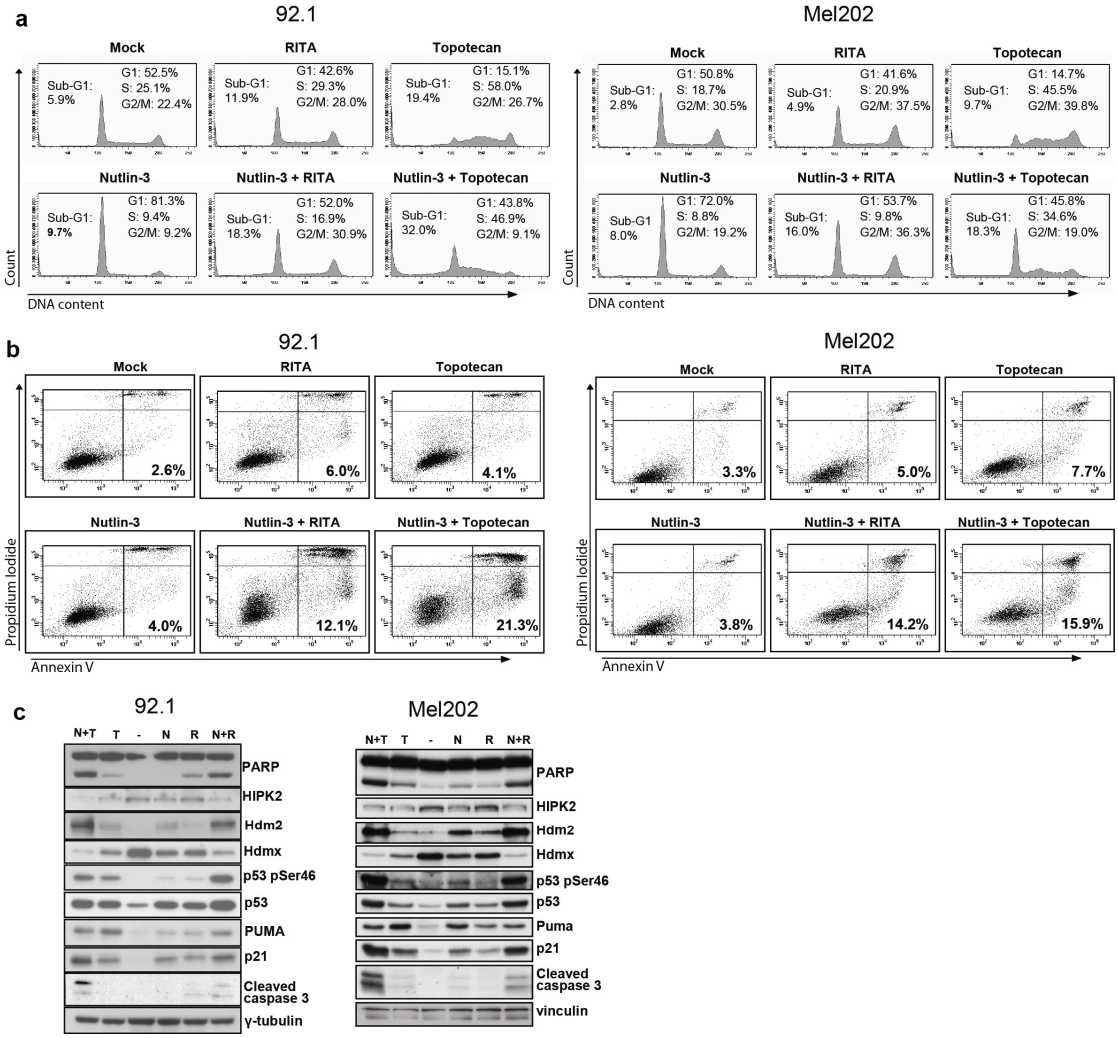

Figure 3 Enhanced apoptosis induction by Nutlin-3 in combination with RITA or Topotecan. Single or combination treatments were performed in 92.1 using 2.0 µM Nutlin-3, 0.7 µM RITA and 25 nM Topotecan and in Mel202 using 3.0 µM Nutlin-3, 0.25 µM RITA and 25 nM Topotecan. (**a**) Flow cytometry analysis after 24 h treatment as indicated. (**b**) Annexin V staining after 48 h treatment as indicated. (**c**) Western blots after 48 h treatment as indicated. N, Nutlin-3; R, RITA; T, Topotecan.

ATM inhibition attenuates p53-Ser46 phosphorylation upon combination treatments without rescuing the induction of apoptosis

We continued the search for the kinase(s) responsible for p53-Ser46 phosphorylation by using a set of specific kinase inhibitors. P53-Ser46 phosphorylation and p53 stabilization was efficiently blocked by Caffeine and by the ATM-specific inhibitor KU55933 (Figure 4a), suggesting a role for the DNA damage sensor kinase ATM. This notion prompted us to investigate the contribution of the DNA damage response more thoroughly. Single Topotecan treatment induced phosphorylation of ATM and its substrates Kap1 and p53-Ser15 (Figure 4b). Addition of Nutlin-3 did not affect p-ATM levels, but slightly reduced p-Kap1, whereas p-p53-Ser15 was elevated in Mel202 cells, correlating with stabilization of p53. Thus, Nutlin-3 might modulate the Topotecan-induced ATM activity. RITA treatment resulted in induction of p-ATM, p-Kap1 and p-p53-Ser15, although to a much lesser extent as compared with Topotecan-treated cells. Combination with Nutlin-3 slightly enhanced ATM and Kap1 phosphorylations in Mel202, but not in 92.1. Increased pSer15-p53 in response to RITA plus Nutlin-3, compared with RITA alone, appears to correlate with extra stabilization of total p53, which is similar to the findings in short-term cultures 08-011 and 10-006 (Supplementary Figure 2).
To investigate the involvement of ATM in more detail, we inhibited ATM activity either by knocking down ATM levels with two different shRNAs (Figures 4c-e), or by using KU55933 (Supplementary Figure 4). Indeed ATM inhibition caused a substantial decrease of the Nutlin-3 plus RITA-induced phosphorylations of p53-Ser15, p53-Ser46, Kap1 and ATM (Figure 4c and Supplementary Figure 4a) as well as the Nutlin-3 plus Topotecan-induced phosphorylations of ATM, Kap1, Chk2, p53-Ser46 and p53-Ser15 (Figure 4d and Supplementary Figure 4b). However, ATM inhibition resulted in even enhanced PARP cleavage, indicating apoptosis induction in the absence of functional ATM. Cell death was confirmed by dramatic increases of sub-G1 cells (Figure 4e and Supplementary Figure 4c). Apparently, inhibiting ATM activity by itself is incompatible with survival of these cells. Therefore, we cannot conclude whether ATM is somehow involved in the mechanism underlying the synergy as found in the combination therapies.

***In vivo* tumor protection by Nutlin-3 and Topotecan**

To investigate the *in vivo* applicability of the treatments, we used mouse melanoma B16F10, a wt-p53 cell line that has frequently been used as model for ocular melanoma, in particular for *in vivo* experiments (Ly *et al.*, 2010). First, we generated stable B16F10 shp53 and shCtrl cell lines to analyze Nutlin-3-mediated p53 activation. In B16-shCtrl, p53 protein

levels and Mdm2 and p21 protein and mRNA levels were induced already after 4 h Nutlin-3 treatment (Supplementary Figure 5a and b), accompanied by reduced cell viability (Supplementary Figure 5c). The observed p53 response and growth inhibition were significantly weaker in B16-shp53, although this was only a partial reduction. Most likely,

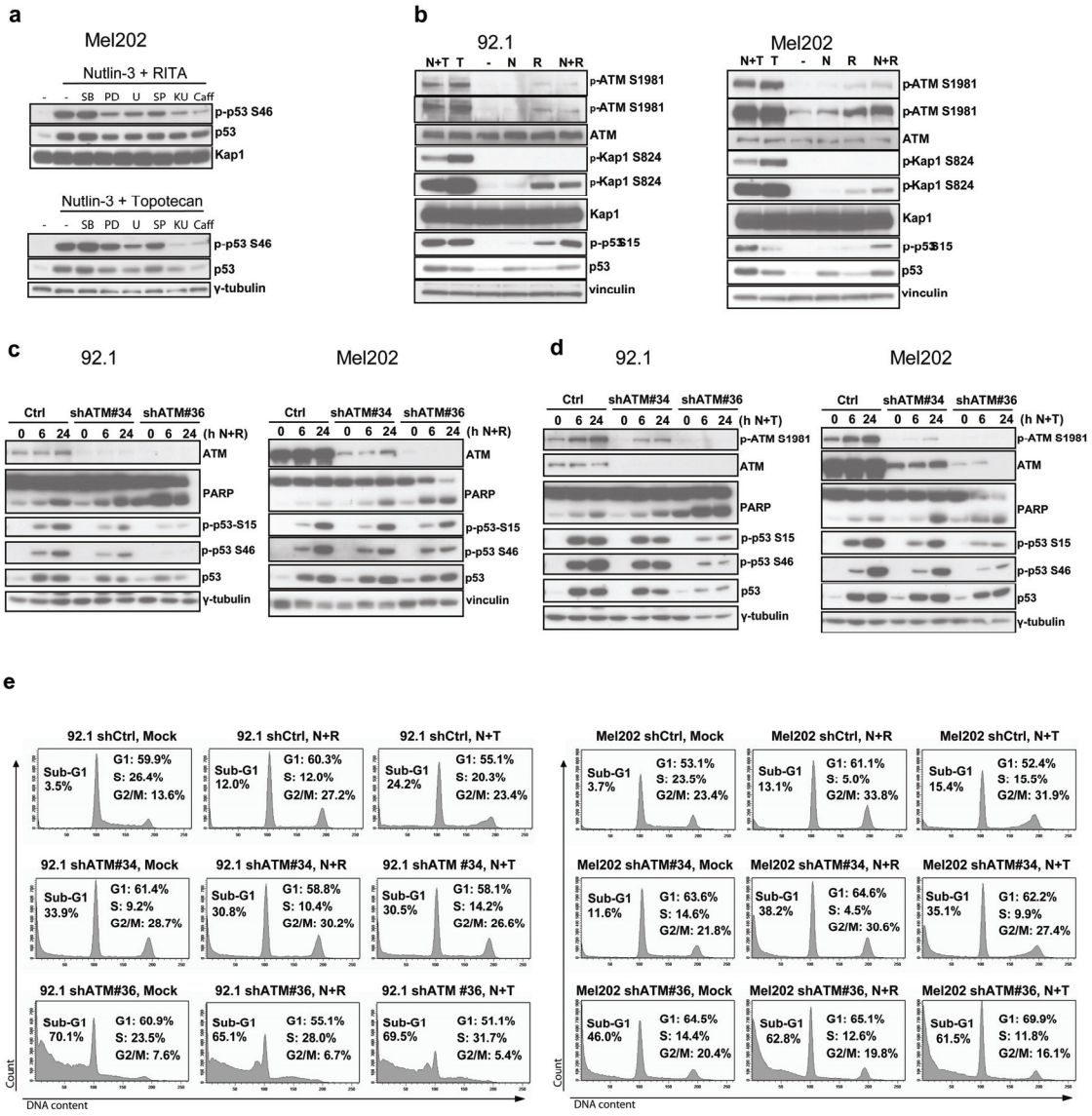

Figure 4 ATM inhibition attenuates p53-Ser46 phosphorylation upon combination treatments without rescuing the induction of apoptosis. (**a**) Western blots of Mel202 cells treated with 3.0 µM Nutlin-3 and 0.25 µM RITA (upper panel) or 3.0 µM Nutlin-3 and 25 nM Topotecan (lower panel) for 24h in the presence of the indicated kinase inhibitors. SB = 10 µM SB203580 (p38 inhibitor), PD = 15 µM PD98059 (MEK1 inhibitor), U = 10 µM U0126 (MEK1 and MEK2 inhibitor), SP = 20 µM SP600125 (JNK1 and JNK2 inhibitor), KU = 10 µM KU55933 (ATM inhibitor), Caff = 10 µM Caffeine (PIKK inhibitor). (**b**) Western blots of 92.1 and Mel202 cells treated for 24 h as in Figure 3. (**c, d**) The 92.1 and Mel202 cells were transduced with shCtrl or shATM RNAs, treated as indicated and analyzed by western blotting. (**e**) Flow cytometry analysis of 92.1 and Mel202 cells transduced with shCtrl or shATM RNAs and treated for 24 h as indicated.

this is because of incomplete p53 knockdown that still enables Nutlin-3 to elicit a reduced effect. We also examined the effect of Nutlin-3 on soft agar growth (Supplementary Figure 5d). Mock-treated B16-shCtrl and B16-shp53 formed colonies in soft agar. Nutlin-3 inhibited colony formation of B16-shCtrl, whereas it only partially affected B16-shp53, indicating that inhibition of anchorage-independent growth by Nutlin-3 is mostly mediated via p53.

Because RITA binds murine p53 very inefficiently (Issaeva *et al.*, 2004), we could only investigate the use of Topotecan in B16F10. Combination of Nutlin-3 and Topotecan resulted in synergistic growth inhibition (Figure 5a) and enhanced p53 activation (Figure 5b). Analogous to the cell cycle profiles in human uveal melanomas (Figure 3a and Supplementary Figure 3), in B16F10 we also observed Nutlin-3-induced G1 arrest, Topotecan-induced G2 arrest and upon combination treatment an additional peak in (late) S-phase, possibly a 'sub-G2' fraction (Figure 5c). Importantly, the sub-G1 fraction was higher after combination treatment compared with single treatments. Next, we used a murine model for ocular melanoma, in which B16F10 cells are injected into the anterior eye chamber (AC) of C57Bl/6 mice. Cells started to form tumors 6-8 days after implantation. Survival (Figure 5d) is defined as the percentage of mice with <80% tumor occupation in their AC; mice were killed upon exceeding this threshold. Subconjunctival delivery of Nutlin-3, Topotecan, or the combination of both (upper graphs) all delayed tumor growth significantly compared with the control group. Although the combination treatment seemed to inhibit tumor growth slightly more efficiently than either drug alone, these differences were not significant (lower graphs).

Equal sensitivity of uveal melanoma cells to treatments under normoxia and hypoxia

At certain stages during tumor development tumor cells are confronted with low-oxygen conditions, which may influence drug sensitivity (Moeller *et al.*, 2005). We investigated responses to the various treatments during hypoxia in 92.1 (Figure 6) and Mel202 (Supplementary Figure 6). Culturing shCtrl and shp53 cells in hypoxia (1% O2) resulted in clear induction of HIF-1α and HIF-2α protein levels (Figure 6a and Supplementary Figure 6a) and increased the expression of the HIF target genes *VEGF*, *Glut1* and *Enolase-γ* (Figure 6b and Supplementary Figure 6b, left panels). These activations appear to be p53 independent, as we observed no major differences between shCtrl and shp53 cells. As expected, Nutlin-3 treatment induced p53 protein levels and enhanced p21, Hdm2 and PUMA protein and mRNA levels in shCtrl, but not in shp53 (Figure 6a and Supplementary Figure 6a and right panels of Figure 6b and Supplementary Figure 6b). Hdmx protein levels

were downregulated upon Nutlin-3 treatment in a p53-dependent manner, as observed in other cell lines (Patton *et al.*, 2006; Wade *et al.*, 2006). Importantly, the inductions of p53, Hdm2, p21 and PUMA by Nutlin-3 were comparable under normoxic and hypoxic conditions.

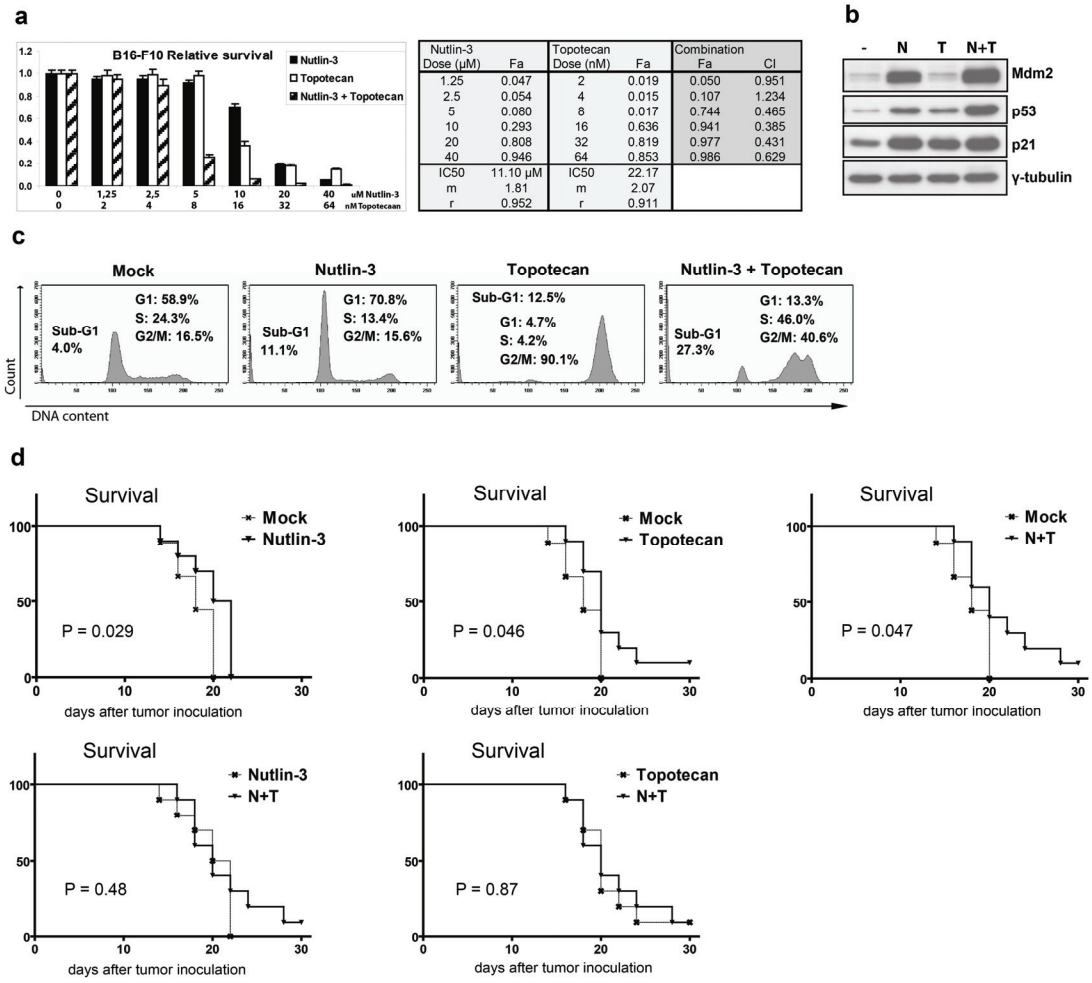

Nutlin-3 Dose (μM)	Fa	Topotecan Dose (nM)	Fa	Combination Fa	CI
1.25	0.047	2	0.019	0.050	0.951
2.5	0.054	4	0.015	0.107	1.234
5	0.080	8	0.017	0.744	0.465
10	0.293	16	0.636	0.941	0.385
20	0.808	32	0.819	0.977	0.431
40	0.946	64	0.853	0.986	0.629
IC50	11.10 μM	IC50	22.17		
m	1.81	m	2.07		
r	0.952	r	0.911		

Figure 5 B16F10 growth inhibition in cell culture and *in vivo* by Nutlin-3 and Topotecan. (**a**) B16F10 cells were counted and seeded for WST-1 proliferation assay. Cells were treated as indicated with different concentrations, alone or in constant ratio combinations, of Nutlin-3 and Topotecan. Cell viability was measured after 72 h treatment, and the effects of drug treatments as fraction of untreated control cells were calculated. The dose-response values IC50, *m* and *r* for each single drug as well as the CI for each drug combination were derived using Compusyn software (Chou and Martin, 2007). CI<0.9, synergy; 0.9<CI<1.1, additive effect; CI>1.1, antagonism. (**b**) Western blot of B16F10 cells treated for 24 h as indicated. N= 10 μM Nutlin-3; T = 25 nM Topotecan. (**c**) Flow cytometry of B16F10 cells treated for 24 h as indicated. (**d**) B16F10 cells were injected into the AC of C57BL/6 mice and animals were either mock treated or treated as described. *In vivo* tumor growth was monitored every 2 days and mice were killed when the AC was filled for 80-100% with tumor cells. The Kaplan-Meyer curves represent percentage survival, defined as the percentage of mice that have <80% tumor occupation in their AC. Log-rank tests were used to determine statistically significant differences between two curves.

We also applied RITA and Topotecan treatments, alone or with Nutlin-3, in hypoxia. At the RITA concentrations we used, no downregulation of HIF-1α was observed in 92.1 and Mel202 cells, in contrast to what was previously described for HCT116 cells (Yang *et al.*, 2009). Interestingly, HIF-1α protein levels were clearly lower in cells treated with Topotecan or with either combination, which partially seemed to correlate with increased levels of HIF-2α (Figure 6c and Supplementary Figure 6c). At mRNA level, the hypoxic inductions of Glut1 (in both cells) and VEGF (Mel202) were unaffected by the treatments, whereas Enolase-γ (in both cells) and VEGF (in 92.1) loosely followed the same trend as HIF-1α protein levels (Figure 6d and Supplementary Figure 6d, left panels). These data suggest that HIF-2α may partially compensate for loss of HIF-1α activity. In line with the results obtained with Nutlin-3 treatment in hypoxia, also RITA, Topotecan and the combination treatments led to comparable inductions of p53, Hdm2, p21 and PUMA in normoxia and hypoxia (Figure 6c, Supplementary Figure 6c and right panels of Figure 6d and Supplementary Figure 6d). Thus, in uveal melanoma cell lines, p53 activation by Nutlin-3, RITA and Topotecan is independent of oxygen level, and is not impaired by altered levels of HIF-1α and HIF-2α. In addition, in B16F10 cells Nutlin-3 was equally efficient in stabilizing p53 and activating Mdm2 and p21 in normoxia and hypoxia (Supplementary Figure 7).

We further investigated the biological treatment responses in hypoxia. Nutlin-3 induced similar growth inhibition in hypoxia and normoxia (Figure 6e and Supplementary Figure 6e). Flow cytometry (Figure 6f and Supplementary Figure 6f) showed that incubation at 1% O_2 for 48h slightly increased G1 fractions, which was p53 dependent (not shown) indicating that hypoxia alone may indeed trigger a minor p53 response (An *et al.*, 1998). All single or combination treatments induced similar patterns when comparing cell cycle profiles in normoxia and hypoxia. Altogether, these data indicate that Nutlin-3, RITA and Topotecan lead to efficient p53 activation in normoxia and hypoxia. This should allow the efficient treatment of cells growing in hypoxic tumor areas.

Discussion

For developing novel cancer therapies, much work has focused on specific reactivation of p53, which is functionally inactivated in virtually all human tumors. About half of the tumors still express a wt-p53 protein that might be reactivated by chemotherapeutic agents. The design of non-genotoxic, small-molecule compounds is potentially attractive as they may target tumors without severely damaging healthy tissues. Uveal melanoma is an example of a cancer generally lacking p53 mutations. Therefore, we investigated the use of

p53-activating drugs as treatment for uveal melanoma. Nutlin-3 specifically disrupts the Hdm2-p53 interaction and has already shown therapeutic potential in both *in vitro* and *in vivo* experiments (Vassilev *et al.*, 2004). In our studies, Nutlin-3 efficiently induced p53-dependent growth inhibition in uveal melanoma cell lines, confirming the presence of wt-p53 and intact down-stream signaling. Interestingly, both 92.1 and Mel202 over-express Hdmx, which is probably responsible for p53 inactivation in these tumor cells. Compared with other uveal melanoma cell lines with low Hdmx, 92.1 and Mel202 showed similar

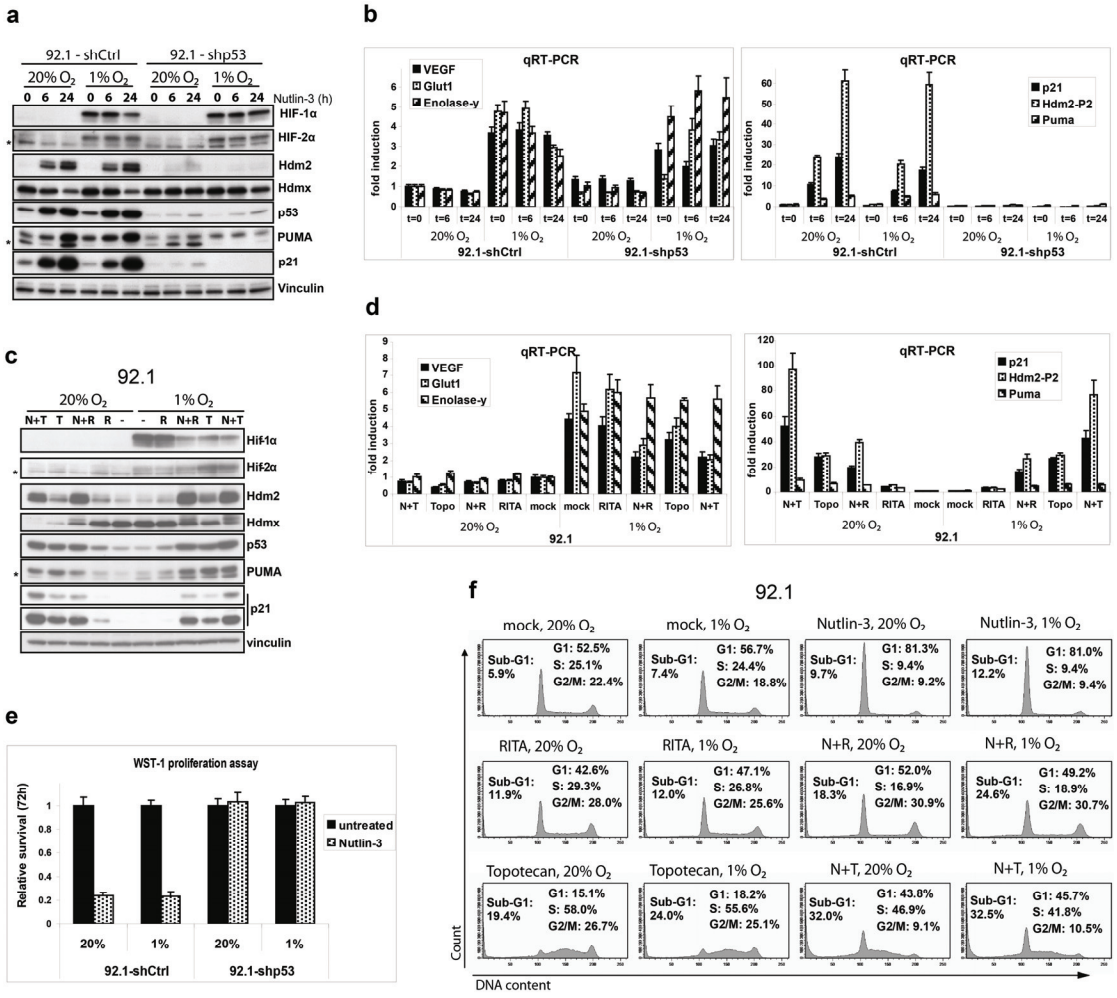

Figure 6 Similar p53 activation and growth inhibition in normoxia and hypoxia by Nutlin-3, RITA and Topotecan in 92.1 cells. The 92.1 cells stably expressing shCtrl or shp53 RNAs were incubated at 20% or 1% O_2 for 48 h and treated with 10 μM Nutlin-3 during the last 6 or 24 h as indicated, followed by western blot analysis (**a**) and qRT-PCR (**b**). Single or combination treatments (24 h) in 92.1 cells incubated at 20% or 1% O_2 for 48 h were performed as indicated using 2.0 μM Nutlin-3, 0.7 μM RITA and 25 nM Topotecan, followed by western blot analysis (**c**) and qRT-PCR (**d**). *Non-specific background staining. (**e**) The 92.1 cells stably expressing shCtrl or shp53 RNAs were counted and seeded for WST-1 proliferation assay. Cells were incubated at 20 or 1% O_2 as indicated, treated with 10 μM Nutlin-3 and cell viability was measured 72 h after treatment. (**f**) The 92.1 cells were incubated at 20 or 1% O_2 for 48 h and treated as indicated during the last 24 h, followed by flow cytometry analysis. Concentrations used: 2.0 μM Nutlin-3, 0.7 μM RITA and 25 nM Topotecan.

sensitivity to Nutlin-3, re-evaluating the idea that Hdmx expression *per se* is an important determinant for the efficacy of Nutlin-3 treatment (Patton *et al.*, 2006; Wade *et al.*, 2006; Hu *et al.*, 2006).

Because p53 can induce both cell cycle arrest and apoptosis, it is crucial to direct the cellular response toward the clinically more desirable apoptosis. In many cell types, however, including the uveal melanoma cells we examined, Nutlin-3 mainly induces G1 arrest. Nutlin-3 may be more effective when used in combination therapy, which ideally results in synergistic growth inhibition. Furthermore, this may reduce the dosage of genotoxic drugs (thus minimizing side effects) and decrease the chance of resistance-conferring mutations. In this study, we show that Nutlin-3 synergizes with both the topoisomerase I inhibitor Topotecan and with the small-molecule p53-activator RITA to inhibit uveal melanoma growth. Importantly, synergy was observed in established cell lines as well as in short-term cultures. The biological basis for synergistic growth inhibition is presumably enhanced apoptosis induction, evidenced by increased sub-G1 fractions, Annexin V staining and cleaved PARP and Caspase 3 levels. How this is achieved mechanistically is more speculative. A potential clue could be the enhanced phosphorylation of p53-Ser46, believed to result in apoptosis induction. Despite earlier reports that RITA activates HIPK2 by reducing Hdm2 (Rinaldo *et al.*, 2009), possibly contributing to RITA-induced apoptosis, we found no evidence for HIPK2 involvement in these cells. Nutlin-3 either alone or in combination with RITA, but not RITA alone, slightly reduced HIPK2 protein levels. HIPK2 reduction correlated with Hdm2 increase, but also with enhanced p53-Ser46 phosphorylation, indicating that a kinase other than HIPK2 is responsible for p53-S46 phosphorylation.

A quick search for the kinase(s) responsible for p53-Ser46 phosphorylation suggested a role for the DNA damage sensor kinase ATM. Several factors support a putative involvement of the DNA damage response. First, multiple kinases involved in p53-Ser46 phosphorylation, including ATM (Saito *et al.*, 2002; Kodama *et al.*, 2010), are induced by DNA damage. Moreover, Topotecan directly leads to double strand-breaks. Recently, also RITA has been indicated to induce a DNA damage response, via a p53-dependent mechanism (Yang *et al.*, 2009). We also found RITA induced phosphorylation of ATM, Kap1 and p53-Ser15, although these were much weaker compared with those induced by Topotecan, when the drugs were used at around IC50 concentrations. Precisely how RITA acts mechanistically remains poorly understood, but its activity clearly stretches beyond p53 stabilization. It is interesting to note that, although both were developed as p53-activating molecules, Nutlin-3 and RITA have very different effects on the cell cycle (G1 vs G2 arrest). This may be an important contribution to the synergy, as only a stronger

activation of the same pathway would be expected to be additive, not synergistic. The involvement of ATM in p53-Ser46 phosphorylation was confirmed by drugs and shRNAs. However, ATM inhibition was incompatible with survival, suggesting that these cells are sensitive to loss of checkpoint activation. Such effects of ATM inhibition have also been described by others (White *et al.*, 2008; Li and Yang 2010). Although by itself this is an intriguing observation and may provide another starting point for developing anti-cancer strategies, it prevents us from concluding whether ATM is involved in the synergy as found in the combination therapies. Further research is necessary to address the relevance of p53-Ser46 phosphorylation. It is noteworthy that also the MEK-inhibitors and the JNK inhibitor affected p53-Ser46 phosphorylation, although less than caffeine or KU55933. It indicates that multiple pathways are activated upon RITA and Topotecan treatment, which might collaborate to obtain the observed biological effects.

For *in vivo* testing of the treatments we switched to mouse melanoma B16F10, given its ability to form tumors when injected into the AC of murine eyes (Ly *et al.*, 2010). Because RITA has very low affinity for mouse p53, we only investigated the use of Nutlin-3 and Topotecan in this model. We confirmed efficient p53 activation by Nutlin-3 and showed synergistic growth inhibition by Nutlin-3 and Topotecan in B16F10. Importantly, both Nutlin-3 and Topotecan delayed *in vivo* tumor growth, albeit only limited. Combination treatment seemed to inhibit tumor growth slightly more efficient, although this trend was not significant. Possibly the experimental conditions need to be further optimized to achieve clear synergy. An important issue may be the fact that drug synergy can be dose dependent. The *in vitro* synergy studies already indicated that in 92.1 and B16F10, Nutlin-3 and Topotecan did not synergize at very low doses. Thus, if the drug delivery in our experimental settings was not sufficient, no synergy might be expected. Final drug concentrations in tumors are difficult to control. When drugs are over-diluted or washed away too quickly, cells will hardly be affected. A solution might be the use of intra-cameral instead of subconjunctival injections.

Notably, our experiment protocol forced us to stop treatments after day 10 following tumor cell inoculation. Around this time-point, the tumors in the combination treatment group were indeed much smaller. Possibly, even the combination treatment does not kill all tumor cells, and upon ending the treatments the surviving cells start growing and initial group differences are lost.

As most tumors at a certain stage face a hypoxic environment, any treatment must be still functional under hypoxic conditions. We mimicked this by culturing cells in 1% O_2 and

found that Nutlin-3, RITA and Topotecan, as well as both combination treatments, induced p53 and subsequent growth inhibition that was equally efficient as in cells cultured at 20% O_2. This predicts that fluctuating oxygen levels *in vivo* will not interfere with the efficacy of the proposed treatments.

Several other investigators examined whether small-molecule activation of p53 potentially mediates anti-angiogenic effects via attenuating HIF-1α mediated transcription. The interplay between the p53 and HIF pathways is not entirely clear. HIF-1α may stabilize p53 through inhibition of Hdm2-mediated p53 ubiquitination (An *et al.*, 1998); in turn, p53 may destabilize HIF-1α by promoting Hdm2-mediated HIF-1α ubiquitination (Ravi *et al.*, 2000). In contrast, direct association of Hdm2 with HIF-1α would increase HIF-1α activity (LaRusch *et al.*, 2007). The use of Nutlin-3 might, therefore, result in p53-dependent degradation of HIF-1α and/ or p53-independent inactivation of HIF-1α by preventing interaction with Hdm2 (Lee *et al.*, 2009). However, we found no evidence for direct inhibition of the hypoxic induction of HIF-1α by Nutlin-3 alone. Perhaps the (impact of Nutlin-3 on) regulation of HIF-1α stability and activity is not universal. A putative direct regulation of HIF-1α by Hdm2 may depend on the cellular context, like high levels of Hdmx as found in the cells we examined. Beside Nutlin-3, also RITA has been implicated in HIF-1α inhibition, supposedly through inducing a DNA damage response and suppressing protein synthesis via phosphorylation of eIF-2α (Yang *et al.*, 2009). In our experiments, RITA alone did not change HIF-1α levels. However, the combination of RITA and Nutlin-3, as well as Topotecan alone or in combination with Nutlin-3, indeed decreased HIF-1α protein levels. These findings would fit into a model in which a certain level of DNA damage response is required for p53-mediated down-regulation of HIF-1α (Kaluzova *et al.*, 2004). Interestingly, HIF-2α seemed to partially compensate for loss of HIF-1α. This implies that for anti-angiogenic therapies also the contribution of HIF-2α needs to be taken into account.

Altogether, our data suggest that synergistic growth inhibition based on small-molecule p53 activation may have clinical potential for ocular melanoma. However, future studies in a clinical setting are necessary to address the utility of p53 activators and possible advantages over the current standard therapies.

Materials and Methods

Cell lines, lentiviral transductions

Human uveal melanoma cell lines 92.1 (De Waard-Siebinga *et al.*, 1995), Mel202, Mel270 and Mel285 and short-term cultures 10-006 and 08-011 were cultured in RPMI + F10 medium (1:1 ratio)

with 10% fetal bovine serum and antibiotics. B16F10 cells were cultured in Dulbecco's modified eagle medium supplemented with 10% fetal bovine serum and antibiotics. Lentiviral constructs (listed in Supplementary Table 1) were described before (Lam *et al.*, 2010) or obtained from the Mission shRNA library (Sigma-Aldrich, St Louis, MO, USA). Cells were transduced using MOI = 1.0 in medium containing 8.0 µg/ml polybrene and puromycin selected for stable expression.

Immunoblotting

Cells were lysed in Giordano buffer (50 mM Tris-HCl, pH 7.4, 250 mM NaCl, 0.1% Triton X-100, 5 mM ethylenediaminetetraacetic acid) with protease- and phosphatase inhibitors. Proteins were separated by sodium dodecyl sulfate-polyacrylamide gel electrophoresis, blotted onto polyvinylidene fluoride transfer membranes, incubated with the appropriate primary (listed in Supplementary Table 2) and secondary antibodies, and bands were visualized by chemoluminescence (West Dura, Pierce Biotechnology, Rockford, IL, USA).

RNA isolation, reverse transcriptase-PCR (RT-PCR)

RNA was isolated using the SV Total RNA isolation kit (Promega, Madison, WI, USA). Complementary DNA was synthesized using 2.0 µg RNA in a total volume of 30 µL reverse transcriptase reaction mixture (Promega). Samples were analyzed in triplicate using SYBR Green mix (Roche Biochemicals, Indianapolis, IN, USA) in a 7900ht Fast Real-Time PCR System (Applied Biosystems, Foster City, CA, USA). For normalization the geometric mean of at least two housekeeping genes was used. Primer sequences are listed in Supplementary Table 3.

Flow cytometry

Cells were harvested, washed in phosphate buffered saline (PBS) and fixed in ice-cold 70% EtOH. Before fluorescence-activated cell sorter analysis, cells were washed in PBS and resuspended in PBS containing 50 µg/mL RNase A and 50 µg/mL propidium iodide. Flow cytometry was performed in the BD LSR II system (BD Biosciences, Sparks, MD, USA). For Annexin V staining, cells were washed twice in PBS and resuspended in Annexin V-binding buffer containing Fluorescein isothyocyanate-labeled Annexin-V (Sigma-Aldrich) and propidium iodide. After 10 min RT incubation cells were analyzed by flow cytometry. Positive propidium iodide staining, indicating necrotic or late apoptotic cells, were excluded from the analysis. Propidium iodide-negative, Annexin V-positive cells represent early apoptotic cells.

WST-1 proliferation assay, calculation of synergism

Cells were counted and seeded in triplicate in 96-well plates at a density of 1500 (B16F10), 3000 (92.1, Mel285 and Mel270) or 6000 (Mel202) cells per well, in a total volume of 100 µL medium. Cells were incubated with 10 µL WST-1 (Roche) for 2 h and absorbance (450 nm) was measured in a microplate reader (Victor; Perkin Elmer, San Jose, CA, USA). For synergy studies, drug effects were calculated as 'affected fraction' of treated vs untreated cells. Dose-effect analyses and calculation of

combination index (CI) were performed using CompuSyn software (Chou and Martin, 2007). CI reflects the extent of synergy or antagonism for two drugs: CI<0.9, synergy; 0.9<CI<1.1, additive effect; CI>1.1, antagonism.

Soft agar assay

Trypsinized cells were counted and resuspended in 0.3% agarose medium containing 10% fetal bovine serum with 10 μM Nutlin-3. 50,000 cells were plated in triplicate over a 0.6% agarose bottom layer with 10 μM Nutlin-3. Medium with Nutlin-3 was replaced every 3-4 days. Colony outgrowth was monitored during 18 days using light microscopy.

***In vivo* tumor growth and treatments**

Authors confirm adherence to the ARVO Statement for use of animals in Ophthalmic and Vision Research. Mice were inoculated with 25,000 cells/ 4 μL B16F10 cells in the anterior chamber (AC) under anaesthesia; a 1:1 mixture of Xylazine (Rompun 2%, Bayer, Leverkussen, Germany) and Ketamine Hydrochloride (Aescoket, Aesculaap bv, Boxtel, The Netherlands), given intraperitoneally. A previously described technique for deposition of tumor cells into the AC was applied (Ly *et al.*, 2010). Treatment was performed on days 2, 4, 6, 8 and 10 after tumor inoculation by subconjunctival injection of 16 μl PBS, 16 μl 100 μM Nutlin-3, or 16 μl 200nM Topotecan, or of 16 μl combination of both drugs, in four different subconjunctival sites, creating a bleb. The eyes were examined every 2 days under a dissecting microscope and tumor volume was recorded as percentage of AC occupied by tumor. Mice were killed when the tumor occupied 80–100% of the AC.

Acknowledgements

We thank Dr PA van der Velden and M Versluis for the primer sets to detect the expression of the HIF target genes and the early cultures of primary uveal melanoma cells, Dr A Vertegaal for the antibodies detecting HIF-1α and HIF-2α proteins, Prof BR Ksander for providing the Mel cell lines, Dr G Selivanova for providing RITA and Dr A Levine for providing anti-Mdm2 antibody. This study was supported by grants from Netherlands Organization for Scientific Research NWO (Mozaiek grant 017.003.059) and by EC FP6 funding (contract 503576).

Reference List

An WG, Kanekal M, Simon MC, Maltepe E, Blagosklonny MV, Neckers LM. (1998). Stabilization of wild-type p53 by hypoxia-inducible factor 1alpha. *Nature* **392;** 405-408.

Augsburger JJ, Correa ZM, Shaikh AH. (2009). Effectiveness of treatments for metastatic uveal melanoma. *Am J Ophthalmol* **148;** 119-127.

Barbieri E, Mehta P, Chen Z, Zhang L, Slack A, Berg S *et al*. (2006). MDM2 inhibition sensitizes neuroblastoma to chemotherapy-induced apoptotic cell death. *Mol Cancer Ther* **5;** 2358-2365.

Bulavin DV, Saito S, Hollander MC, Sakaguchi K, Anderson CW, Appella E *et al*. (1999). Phosphorylation of human p53 by p38 kinase coordinates N-terminal phosphorylation and apoptosis in response to UV radiation. *EMBO J* **18;** 6845-6854.

Chang AE, Karnell LH, Menck HR. (1998). The National Cancer Data Base report on cutaneous and noncutaneous melanoma: a summary of 84,836 cases from the past decade. The American College of Surgeons Commission on Cancer and the American Cancer Society. *Cancer* **83;** 1664-1678.

Chou TC. (2006). Theoretical basis, experimental design, and computerized simulation of synergism and antagonism in drug combination studies. *Pharmacol Rev* **58;** 621-681.

Chou, T. C. and Martin, N. CompuSyn software for drug combinations and for general dose-effect analysis, and user's guide. 9-2-2007. ComboSyn, Inc.Paramus, NJ. 2007.
Ref Type: Computer Program

Coll-Mulet L, Iglesias-Serret D, Santidrian AF, Cosialls AM, de FM, Castano E *et al*. (2006). MDM2 antagonists activate p53 and synergize with genotoxic drugs in B-cell chronic lymphocytic leukemia cells. *Blood* **107;** 4109-4114.

D'Orazi G, Cecchinelli B, Bruno T, Manni I, Higashimoto Y, Saito S *et al*. (2002). Homeodomain-interacting protein kinase-2 phosphorylates p53 at Ser 46 and mediates apoptosis. *Nat Cell Biol* **4;** 11-19.

De Waard-Siebinga I, Blom DJ, Griffioen M, Schrier PI, Hoogendoorn E, Beverstock G *et al*. (1995). Establishment and characterization of an uveal-melanoma cell line. *Int J Cancer* **62;** 155-161.

Enge M, Bao W, Hedstrom E, Jackson SP, Moumen A, Selivanova G. (2009). MDM2-dependent downregulation of p21 and hnRNP K provides a switch between apoptosis and growth arrest induced by pharmacologically activated p53. *Cancer Cell* **15;** 171-183.

Hu B, Gilkes DM, Farooqi B, Sebti SM, Chen J. (2006). MDMX overexpression prevents p53 activation by the MDM2 inhibitor Nutlin. *J Biol Chem* **281;** 33030-33035.

Issaeva N, Bozko P, Enge M, Protopopova M, Verhoef LG, Masucci M *et al*. (2004). Small molecule RITA binds to p53, blocks p53-HDM-2 interaction and activates p53 function in tumors. *Nat Med* **10;** 1321-1328.

Kaluzova M, Kaluz S, Lerman MI, Stanbridge EJ. (2004). DNA damage is a prerequisite for p53-mediated proteasomal degradation of HIF-1alpha in hypoxic cells and downregulation of the hypoxia marker carbonic anhydrase IX. *Mol Cell Biol* **24;** 5757-5766.

Kivela T, Eskelin S, Kujala E. (2006). Metastatic uveal melanoma. *Int Ophthalmol Clin* **46;** 133-149.

Kodama M, Otsubo C, Hirota T, Yokota J, Enari M, Taya Y. (2010). Requirement of ATM for rapid p53 phosphorylation at Ser46 without Ser/Thr-Gln sequences. *Mol Cell Biol* **30;** 1620-1633.

Kojima K, Konopleva M, McQueen T, O'Brien S, Plunkett W, Andreeff M. (2006). Mdm2 inhibitor Nutlin-3a induces p53-mediated apoptosis by transcription-dependent and transcription-independent mechanisms and may overcome Atm-mediated resistance to fludarabine in chronic lymphocytic leukemia. *Blood* **108;** 993-1000.

Krajewski M, Ozdowy P, D'Silva L, Rothweiler U, Holak TA. (2005). NMR indicates that the small molecule RITA does not block p53-MDM2 binding in vitro. *Nat Med* **11;** 1135-1136.

Lam S, Lodder K, Teunisse AF, Rabelink MJ, Schutte M, Jochemsen AG. (2010). Role of Mdm4 in drug sensitivity of breast cancer cells. *Oncogene*.

LaRusch GA, Jackson MW, Dunbar JD, Warren RS, Donner DB, Mayo LD. (2007). Nutlin3 blocks vascular endothelial growth factor induction by preventing the interaction between hypoxia inducible factor 1alpha and Hdm2. *Cancer Res* **67;** 450-454.

Laurie NA, Donovan SL, Shih CS, Zhang J, Mills N, Fuller C *et al*. (2006). Inactivation of the p53 pathway in retinoblastoma. *Nature* **444;** 61-66.

Lee YM, Lim JH, Chun YS, Moon HE, Lee MK, Huang LE *et al*. (2009). Nutlin-3, an Hdm2 antagonist, inhibits tumor adaptation to hypoxia by stimulating the FIH-mediated inactivation of HIF-1alpha. *Carcinogenesis* **30;** 1768-1775.

Li Y, Yang DQ. (2010). The ATM inhibitor KU-55933 suppresses cell proliferation and induces apoptosis by blocking Akt in cancer cells with overactivated Akt. *Mol Cancer Ther* **9;** 113-125.

Ly LV, Baghat A, Versluis M, Jordanova ES, Luyten GP, van RN *et al*. (2010). In aged mice, outgrowth of intraocular melanoma depends on proangiogenic M2-type macrophages. *J Immunol* **185;** 3481-3488.

Moeller BJ, Dreher MR, Rabbani ZN, Schroeder T, Cao Y, Li CY *et al*. (2005). Pleiotropic effects of HIF-1 blockade on tumor radiosensitivity. *Cancer Cell* **8;** 99-110.

Patton JT, Mayo LD, Singhi AD, Gudkov AV, Stark GR, Jackson MW. (2006). Levels of HdmX expression dictate the sensitivity of normal and transformed cells to Nutlin-3. *Cancer Res* **66;** 3169-3176.

Ravi R, Mookerjee B, Bhujwalla ZM, Sutter CH, Artemov D, Zeng Q *et al*. (2000). Regulation of tumor angiogenesis by p53-induced degradation of hypoxia-inducible factor 1alpha. *Genes Dev* **14;** 34-44.

Rinaldo C, Prodosmo A, Siepi F, Moncada A, Sacchi A, Selivanova G *et al*. (2009). HIPK2 regulation by MDM2 determines tumor cell response to the p53-reactivating drugs nutlin-3 and RITA. *Cancer Res* **69;** 6241-6248.

Saito S, Goodarzi AA, Higashimoto Y, Noda Y, Lees-Miller SP, Appella E *et al*. (2002). ATM mediates phosphorylation at multiple p53 sites, including Ser(46), in response to ionizing radiation. *J Biol Chem* **277;** 12491-12494.

Tomicic MT, Christmann M, Kaina B. (2010). Topotecan triggers apoptosis in p53-deficient cells by forcing degradation of XIAP and survivin thereby activating caspase-3-mediated Bid cleavage. *J Pharmacol Exp Ther* **332;** 316-325.

Vassilev LT. (2007). MDM2 inhibitors for cancer therapy. *Trends Mol Med* **13;** 23-31.

Vassilev LT, Vu BT, Graves B, Carvajal D, Podlaski F, Filipovic Z *et al*. (2004). In vivo activation of the p53 pathway by small-molecule antagonists of MDM2. *Science* **303;** 844-848.

Wade M, Wong ET, Tang M, Stommel JM, Wahl GM. (2006). Hdmx modulates the outcome of p53 activation in human tumor cells. *J Biol Chem* **281;** 33036-33044.

White JS, Choi S, Bakkenist CJ. (2008). Irreversible chromosome damage accumulates rapidly in the absence of ATM kinase activity. *Cell Cycle* **7;** 1277-1284.

Wynford-Thomas D, Blaydes J. (1998). The influence of cell context on the selection pressure for p53 mutation in human cancer. *Carcinogenesis* **19;** 29-36.

Yang J, Ahmed A, Poon E, Perusinghe N, de Haven BA, Box G *et al*. (2009). Small-molecule activation of p53 blocks hypoxia-inducible factor 1alpha and vascular endothelial growth factor expression in vivo and leads to tumor cell apoptosis in normoxia and hypoxia. *Mol Cell Biol* **29;** 2243-2253.

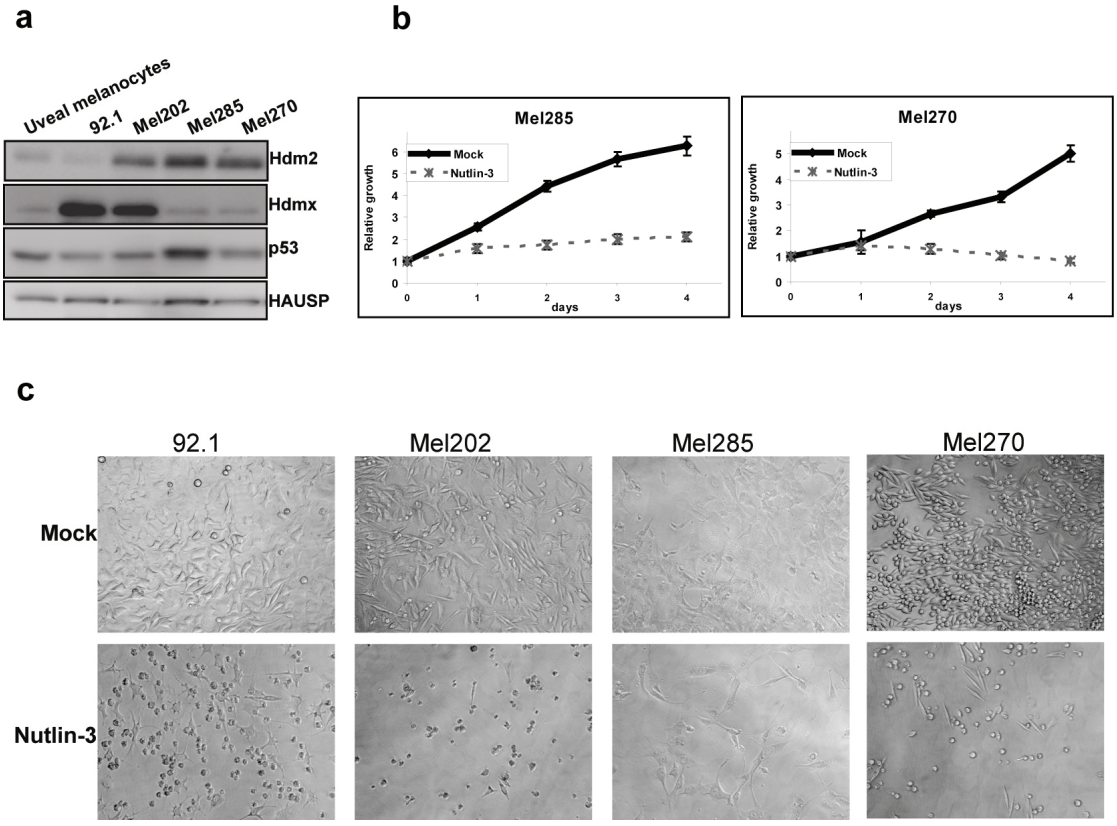

Supplementary Figure 1 No correlation between basal Hdmx and Hdm2 levels and sensitivity to Nutlin-3. (**a**) Four uveal melanoma cell lines and uveal melanocytes as control were analyzed by Western blot for the indicated protein levels. (**b**) Mel285 and Mel270 cells were counted, seeded for WST-1 proliferation assay, and treated with 10 µM Nutlin-3. Cell viability was measured at 0, 24, 48, 72, and 96 h after treatment. (**c**) 72 h after addition of Nutlin-3, pictures were taken from the 96-wells plates from panel (**b**).

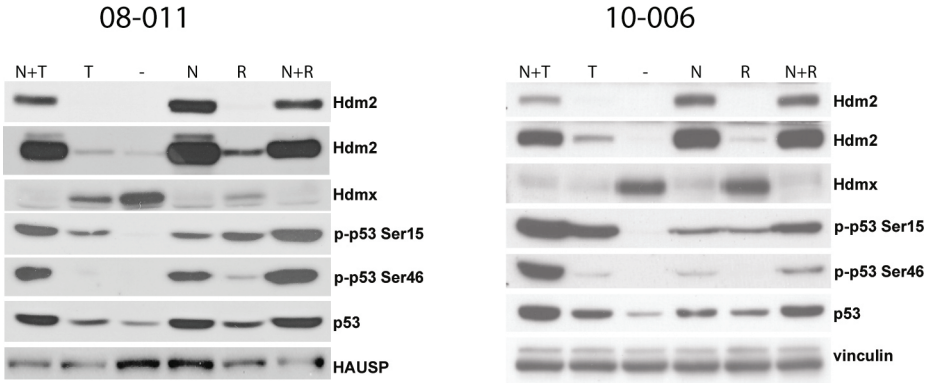

Supplementary Figure 2 Enhanced p53 phosphorylation and stabilization in short-term uveal melanoma cultures upon treatment with Nutlin-3 in combination with RITA or Topotecan. Western blots were performed after 24 h single or combination treatments in short-term uveal melanoma cultures 08-011 and 10-006 as indicated. Treatments in 08-011: N, 12 µM Nutlin-3; R, 0.2 µM RITA; T, 100 nM Topotecan. Treatments in 10-006: N, 8 µM Nutlin-3; R, 1 µM RITA, T, 100 nM Topotecan.

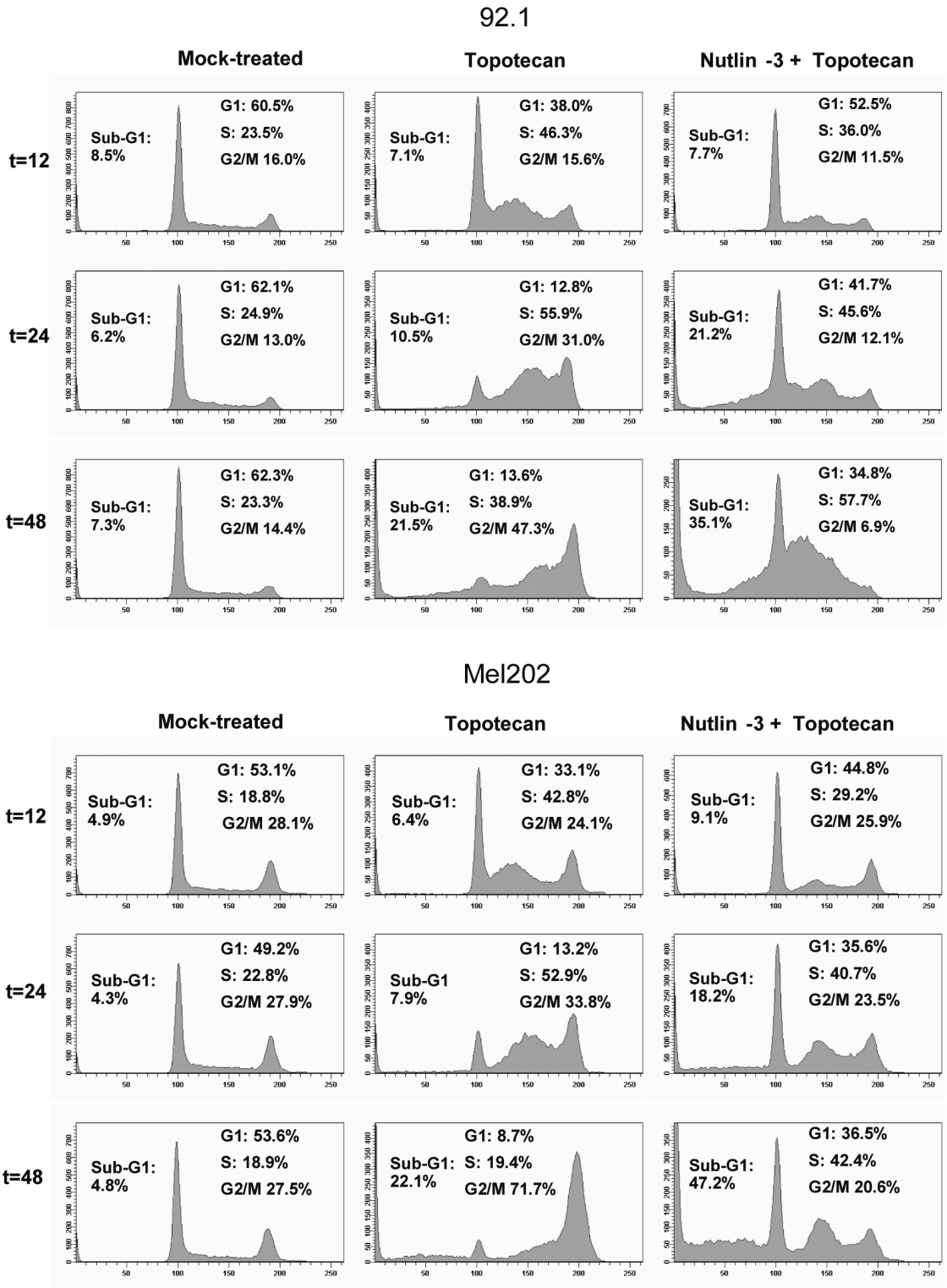

Supplementary Figure 3 Kinetic analysis of the cell cycle in response to Topotecan alone or in combination with Nutlin-3. Flow cytometry analysis of 92.1 and Mel202 cells treated for 12 h, 24 h or 48 h as indicated. Used concentrations in 92.1: 2.0 µM Nutlin-3, 25 nM Topotecan. Used concentrations in Mel202: 3.0 µM Nutlin-3 and 25 nM Topotecan.

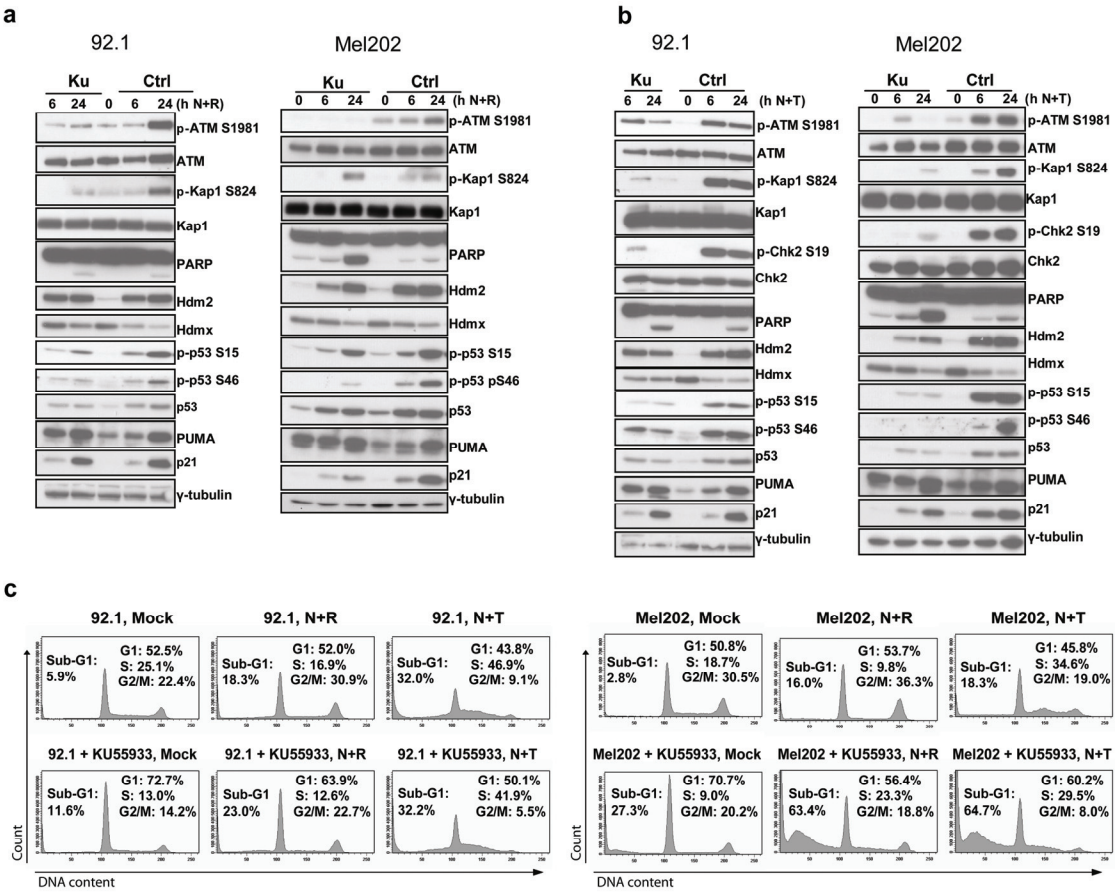

Supplementary Figure 4 ATM inhibition attenuates p53-Ser46 phosphorylation upon combination treatments without rescuing the induction of apoptosis. 92.1 and Mel202 cells were 2 h pre-treated with 10 µM KU55933, treated for 24 h as indicated and analyzed by Western blot (**a**, **b**) and flow cytometry (**c**). Used concentrations in 92.1: 2.0 µM Nutlin-3, 0.7 µM RITA, 25 nM Topotecan. Used concentrations in Mel202: 3.0 µM Nutlin-3, 0.25 µM RITA, 25 nM Topotecan.

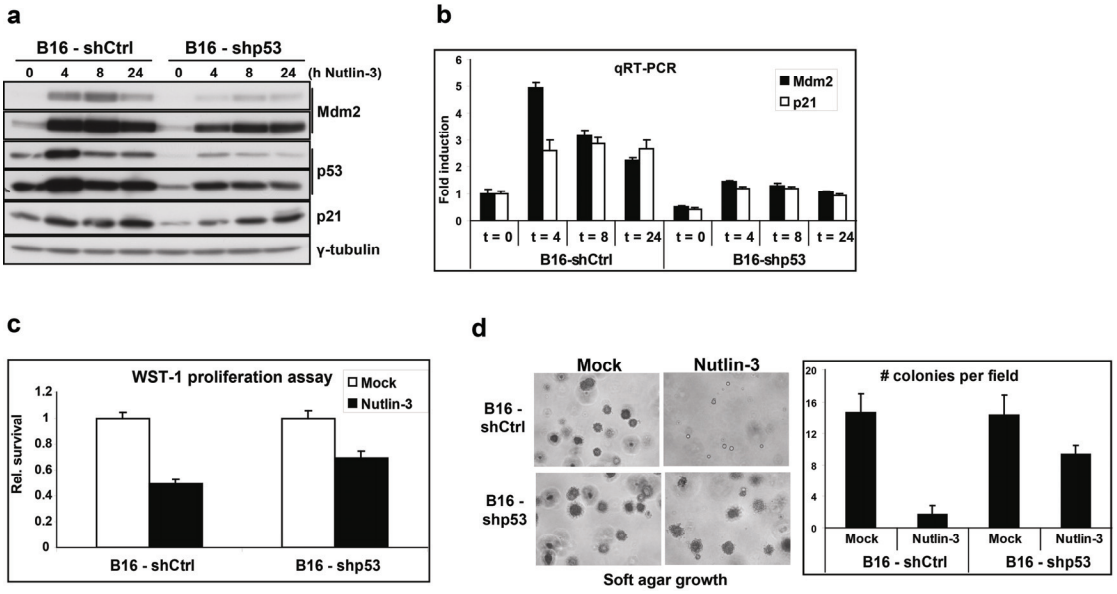

Supplementary Figure 5 Nutlin-3 activates p53 and inhibits cell growth in B16F10 cells. B16F10 cells stably expressing shCtrl or shp53 RNAs were treated with 10 µM Nutlin-3 for the indicated times and analyzed by Western blot (**a**) and qRT-PCR (**b**). (**c**) Cells were counted and seeded for WST-1 proliferation assay and treated with 10 µM Nutlin-3. Cell viability was measured 72 h after treatment. (**d**) B16F10 cells stably expressing shCtrl or shp53 RNAs were counted and seeded in triplicate in soft agar containing 10 µM Nutlin-3. Medium with Nutlin-3 was replaced every 3-4 days. Colony outgrowth was monitored with light microscopy and after 18 days the colonies were counted (one microscope field per well). Representative pictures and a quantification of the results are shown.

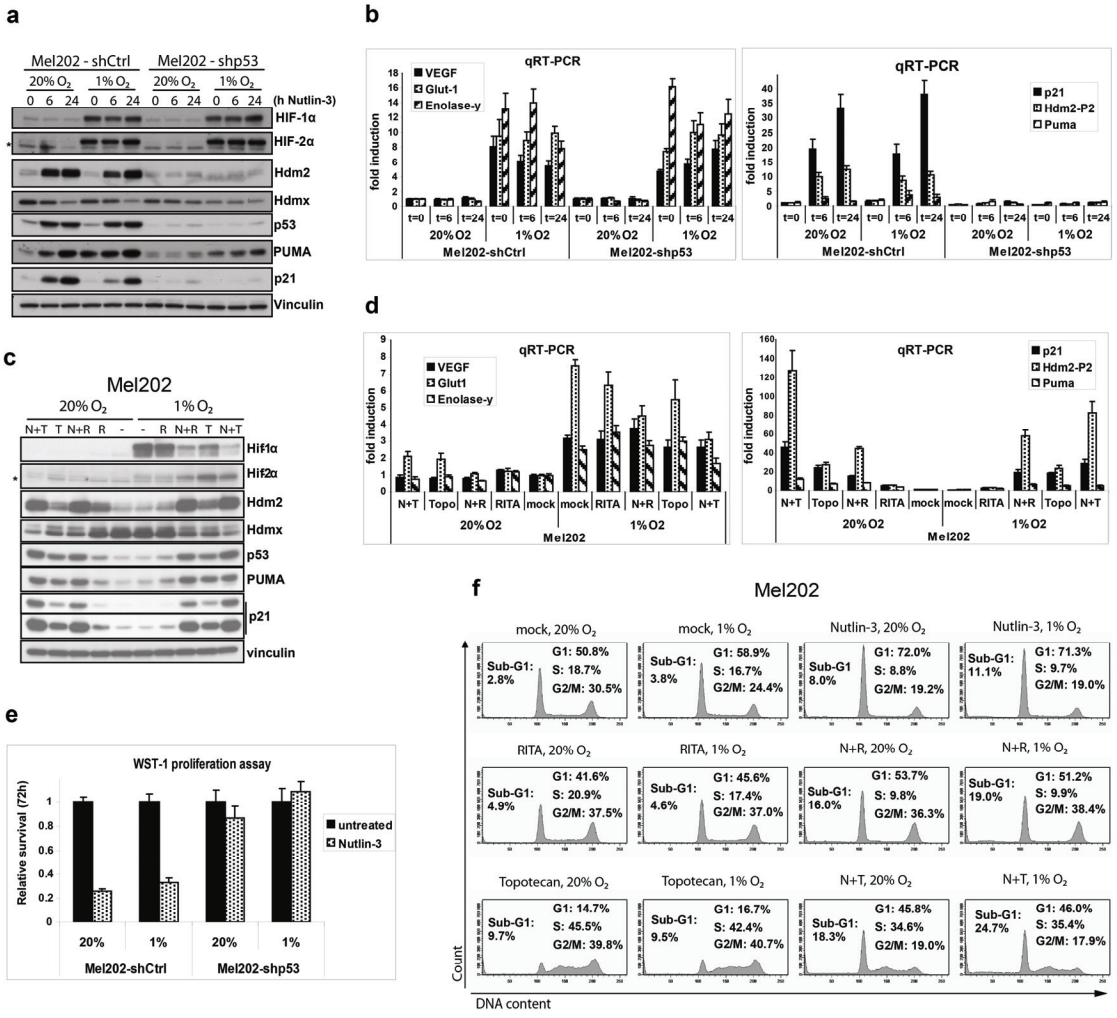

Supplementary Figure 6 Similar p53 activation and growth inhibition in normoxia and hypoxia by Nutlin-3, RITA and Topotecan in Mel202 cells. Mel202 cells stably expressing shCtrl or shp53 RNAs were incubated at 20% or 1% O_2 for 48 h and treated with 10 µM Nutlin-3 during the last 6 or 24 h as indicated, followed by Western blot analysis (**a**) and qRT-PCR (**b**). Single or combination treatments (24 h) in Mel202 cells incubated at 20% or 1% O_2 for 48 h were performed as indicated using 3.0 µM Nutlin-3, 0.25 µM RITA and 25 nM Topotecan, followed by Western blot analysis (**c**) and qRT-PCR (**d**). *Non-specific background staining. (**e**) Mel202 cells stably expressing shCtrl or shp53 RNAs were counted and seeded for WST-1 proliferation. Cells were incubated at 20 or 1% O_2 as indicated, treated with 10 µM Nutlin-3 and cell viability was measured 72 h after treatment. (**f**) The Mel202 cells were incubated at 20% or 1% O_2 for 48 h and treated as indicated during the last 24 h, followed by flow cytometry analysis. Concentrations used: 3.0 µM Nutlin-3, 0.25 µM RITA and 25 nM Topotecan.

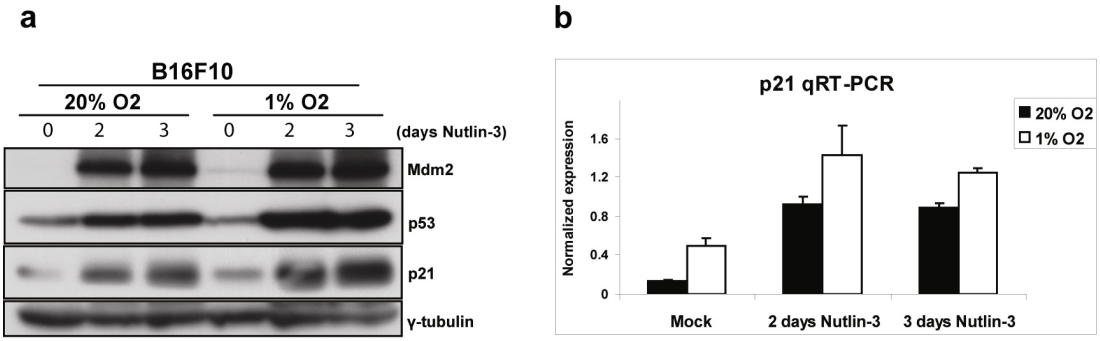

Supplementary Figure 7 Similar Nutlin-3 induced p53 activation under normoxic and hypoxic conditions in B16F10 cells. B16F10 cells were cultured at 1% or 20% O_2 for 72 h and treated with Nutlin-3 for the final 2 or 3 days, followed by Western blot analysis (**a**) and qRT-PCR (**b**).

Supplementary Table 1: List of shRNA sequences

shRNA	Target sequences
human shCtrl	GAATCTTGTTACATCAGCT
human shp53	GACTCCAGTGGTAATCTAC
human shATM #34	CCTTTCATTCAGCCTTTAGAA
human shATM #36	TGATGGTCTTAAGGAACATCT
mouse shCtrl	CGAAATTGGATCACAGCGATA
mouse shp53 #1	CCGACCTATCCTTACCATCAT
mouse shp53 #2	CTACAAGAAGTCACAGCACAT
mouse shp53 #3	CGGGCGTAAACGCTTCGAGAT

Supplementary Table 2: List of antibodies

Protein	Name/ cat. #	Company
Hdmx	A300-287A	Bethyl Laboratories, Montgomery TX, USA
Hdm2 * / Mdm2	4B2	Chen *et al*., 1993
Hdm2 *	SMP14 sc-6965	Santa Cruz Biotechnology, Santa Cruz, CA, USA
p53 °	DO-1 / sc-126	Santa Cruz Biotechnology, Santa Cruz, CA, USA
p53 °	18O1 / sc-98	Santa Cruz Biotechnology, Santa Cruz, CA, USA
mouse p53	1C12 / 2524	Cell signalling Technology, Beverly, MA, USA
p-p53 Ser46	2521	Cell signalling Technology, Beverly, MA, USA
p-p53 Ser15	9284	Cell signalling Technology, Beverly, MA, USA
PUMA N-terminal	P4743	Sigma-Aldrich, St Louis, MO, USA
p21	CP74 / 05-655	Upstate Biotechnology, Lake Placid, NY, USA
mouse p21	F5 / sc-6246	Santa Cruz Biotechnology, Santa Cruz, CA, USA
vinculin	hVIN-1 / V9131	Sigma-Aldrich, St Louis, MO, USA
γ-tubulin	GTU-88 / T6557	Sigma-Aldrich, St Louis, MO, USA
HAUSP USP7	A300-033A	Bethyl Laboratories, Montgomery TX, USA
PARP	9542	Cell signalling Technology, Beverly, MA, USA
cleaved caspase 3 (Asp175)	9661	Cell signalling Technology, Beverly, MA, USA
HIPK2	F-189 / sc-100383	Santa Cruz Biotechnology, Santa Cruz, CA, USA
HIF-1α	610958	BD Biosciences, San Diego, CA, USA
HIF-2α	NB100-122	Novus Biologicals, Littleton, CO, USA
p-ATM S1981	EP1890Y / 2152-1	Epitomics,California, USA
ATM	Y170 / 1549-1	Epitomics,California, USA
p-Kap1 S824	A300-767A	Bethyl Laboratories, Montgomery TX, USA
Kap1	A300-274A	Bethyl Laboratories, Montgomery TX, USA
p-Chk2 S19	2666	Cell signalling Technology, Beverly, MA, USA
Chk2	EPR4325 / 3428-1	Epitomics,California, USA

For detection of human Hdm2 we used a mix of 4B2 and SMP14 (*), for detection of human p53 we used a mix of DO-1 and 1801 (°).

Ref) Chen J *et al.* **Mapping of the p53 and mdm-2 interaction domains**. *Mol Cell Biol* 1993, **13:**4107-4114.

Supplementary Table 3: Primer sequences used for qRT-PCR reactions.

Human gene	Forward primer	Reverse primer
p21	AGCAGAGGAAGACCATGTGGA	AATCTGTCATGCTGGTCTGCC
Hdm2 Exon 2	ACGCACGCCACTTTTTCTCT	TCCGAAGCTGGAATCTGTGAG
PUMA	GACCTCAACGCACAGTA	CTAATTGGGCTCCATCT
VEGF	GCCTTGCCTTGCTGCTCTACC	GTGATGATTCTGCCTCCTCCTTC
Glut1	CCCGCTTCCTGCTCATCAACC	GCCGACTCTCTTCCTTCATCTCC
Enolase-γ	TAGAATGGGAAGGGTCATAGAAAGGG	AGAGGTGGTGGCAACTGTGG
CAPNS1	ATGGTTTTGGCATTGACACATG	GCTTGCCTGTGGTGTCGC
Beta-Actin	CGGGACCTGACTGACTACCTC	CTCCTTAATGTCACGCACGATTTC
ARP	CACCATTGAAATCCTGAGTGATGT	ACCAGCCGAAAGGAGAAG
RPS11	AAGCAGCCGACCATCTTTCA	CGGGAGCTTCTCCTTGCC
Mouse gene	**Forward primer**	**Reverse primer**
p21	CCTGACAGATTTCTATCACTCCA	AGGCAGCGTATATCAGGAG
Mdm2	CGGCCTAAAAATGGTTGCAT	TTTGCACACGTGAAACATGACA
β2-Microglobulin	CGGTCGCTTCAGTCGTCAG	GCAGTTCAGTATGTTCGGCTTCC